Journal of Materials Chemistry C

Accepted Manuscript

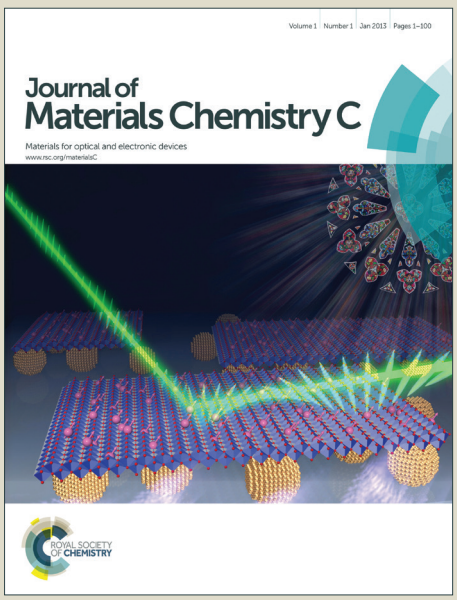

ROYAL SOCIETY OF CHEMISTRY

www.rsc.org/materialsC

GRAPHICAL ABSTRACT

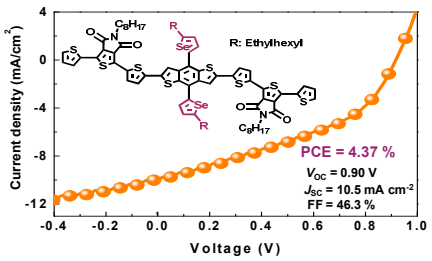

A novel small molecule with alkylselenophene-substituted benzodithiophene unit, **BDTSe-TTPD**, showed strong light absorption, low HOMO level and their photovoltaic characteristics with power conversion efficiency as high as 4.37%.

A high-performing solution-processed small molecule : alkylselenophene-substituted benzodithiophene organic solar cell

Yu Jin Kim[a‡], Jang Yeol Baek [b‡], Jong-jin Ha[b], Dae Sung Chung[d*], Soon-Ki Kwon[b]*, Chan Eon Park[a]* and Yun-Hi Kim[c]*

[a] POSTECH Organic Electronics Laboratory, Department of Chemical Engineering, Pohang University of Science and Technology, Pohang, 790-784, Republic of Korea

[b] School of Materials Science & Engineering and Research Institute for Green Energy Convergence Technology (REGET), Gyeongsang National University, Jin-ju, 660-701, Republic of Korea

[c] Department of Chemistry & ERI, Gyeongsang National University, Jin-ju, 660-701, Republic of Korea

[d] School of Chemical Engineering and Material Science Chung-Ang University, Seoul, 156–756, Republic of Korea

*Corresponding Authors:

1. Prof. Soon-Ki Kwon

School of Materials Science & Engineering and Research Institute for Green Energy Convergence Technology (REGET),

Gyeongsang National University,

Jin-ju, 660-701, Republic of Korea

Email: skwon@gnu.ac.kr

2. Prof. Chan Eon Park

POSTECH Organic Electronics Laboratory,

Department of Chemical Engineering,

Pohang University of Science and Technology,

Pohang, 790-784, Republic of Korea

Email: cep@postech.ac.kr

3. Prof. Yun-Hi Kim

Department of Chemistry & Research Institute of Natural Science,

Gyeongsang National University,

Jin-ju, 660-701, Republic of Korea

Email: ykim@gnu.ac.kr

4. Prof. Dae Sung Chung

School of Chemical Engineering and Material Science,

Chung-Ang University

Seoul, 156–756, Republic of Korea

Email: dchung@cau.ac.kr

Correspondence to: Yun-Hi Kim (E-mail: ykim@gnu.ac.kr)

‡Yu Jin Kim and Jang Yeol Baek contributed equally to this work.

Abstract

A solution-processed alkylselenophene-substituted benzodithiophene (BDT) small molecule, namely, 3,3'-((4,8-bis(5-(2-ethylhexyl)selenophen-2-yl)benzo[1,2-*b*:4,5-*b'*]dithiophene-2,6-diyl)bis(thiophene-5,2-diyl))bis(5-octyl-1-(thiophen-2-yl)-4H-thieno[3,4-*c*]pyrrole-4,6(5H)-dione) (**BDTSe-TTPD)**, with broad absorption and suitable energy levels was synthesized. The widely used solvents *o*-dichlorobenzene (*o*-DCB), chlorobenzene (CB) or chloroform (CF) were used as the spin-coating solvent, to fabricate efficient photovoltaic devices with **BDTSe-TTPD** as the donor material and $PC_{71}BM$ as the acceptor. Devices made from a CF solution demonstrated better performance in terms of short-circuit current, fill factor and power conversion efficiency, as compared to the devices made from the *o*-DCB and CB solutions. Finally, by optimizing the thickness of the active layer, a power conversion efficiency of 4.37% was achieved on devices area of 0.09 cm^2, under 100 mW/cm^2 of simulated AM 1.5 irradiation.

Keywords

Solution-processed small molecule, Alkylselenophene, Benzodithiophene, Organic solar cells, Device optimization

Introduction

Organic photovoltaics (OPVs) are considered to be a promising next-generation green technology to address increasing energy problems worldwide.[1-2] Currently, OPVs are based on conjugated polymers as electron donor materials and have achieved power conversion efficiencies (PCEs) of up to 10%.[3] Meanwhile, small molecule organic solar cells (SMOSCs) are emerging because of their simpler synthesis, lower batch-to-batch variation, and greater reproducibility in solar cell performance.[4-5] To date, state-of-the-art solution-processed SMOSCs have demonstrated PCEs of > 8%,[6] but their overall performance is still significantly behind that of their polymer counterparts.[7] The first step to close this gap in performance is to design better materials in the active layer.

To address this issue, our recently reported molecule TBDT-TTPD containing a central thiophene-substituted benzo[1,2-b:4,5-b′]dithiophene (BDT) unit achieved a high PCE of 4.62% with optimized *V*oc (0.97 V), *J*sc (9.1 mA cm^{-2}) and FF (52 %).[8] The thiophene-substituted BDT unit with a two-dimensional (2-D) conjugated structure imparts very interesting properties and promising photovoltaic performance. Generally, broad and strong absorption bands can be achieved owing to an extended side chain.[9] Also, since 2-D conjugated thiophenes have larger conjugated planes than their one-dimensional conjugated counterparts, better inter-chain –overlapping may be formed, and higher charge mobility can be achieved.[10] Additionally, the selenophene moiety could enhance the inter-chain interactions between compound chains due to strong Se-Se interactions.[11] Furthermore, the inclusion of the selenophene building block could lower the HOMO energy level of the resulting compounds compared to the corresponding thiophene building block.[12] Based on these superior properties, Heeger *et al.* achieved a PCE of 5.30% from alternating copolymer, P(Se), composed of selenophene and thienopyrrole-4,6-dione.[13] Yang and co-workers reported a 4.12% PCE using selenophene-based polymer, PCDSeBT, in which the

diselenienylbenzothiadiazole (DSeBT) monomer alternates with a 2,7-carbazole unit.[14] Therefore synthesis based on a selenophene unit could be very interesting as a new building block for donor materials in OPVs. To the best of our knowledge, selenophene-based small molecule materials have rarely been reported.

In this article, we selected the two-dimensional conjugate unit of benzodithiophene (BDT) with selenophenes as the donor unit, and two TPD units as the acceptor units, both covalently attached to the ends of BDT. Long alkyl side groups were attached to the selenophene moiety to ensure solubility, finally forming **BDTSe-TTPD**, an A-D-A type solution-processed small molecule. On the basis of this molecule, photovoltaic devices were fabricated with *o*-dichlorobenzene (*o*-DCB), chlorobenzene (CB) or chloroform (CF), as the solvents. The results indicated that the devices prepared from *o*-DCB exhibited a low short-circuit current (J_{SC}) and fill factor, owingto the poor morphology and weak compound stacking. When CF was used, the J_{SC} and FF were both improved because of improved nano-scale morphology and well-ordered **BDTSe-TTPD** crystalline domains. Finally, after active layer thickness optimizations, a PCE of 4.37%, with a V_{OC} of 0.90 V, a J_{SC} of 10.5 mA/cm^2, and an FF of 46.3 % was obtained. This PCE is the highest efficiency reported to date for devices prepared using an alkylselenophene-substituted benzodithiophene (BDT) small molecule.

Results and discussion

Synthesis and thermal property

BDTSe-TTPD was synthesized according to Scheme 1. *2*,6-Bis(trimethyltin)-4,8-bis(5-(2-ethylhexyl)selenophen-2-yl)benzo[1,2-b:4,5-b']dithiophene (3) was synthesized by monoalkylation of selenophene, lithiation, nucleophilic addition, reduction and stannylation. 1-(5-Bromothiophen-2-yl)-5-octyl-3-(thiophen-2-yl)-4H-thieno[3,4-c]pyrrole-4,6(5H)-dione (5) was obtained by Stille coupling reaction and bromination. **BDTSe-TTPD** was synthesized

using compound 3 and compound 5, via a Stille coupling reaction. The structure of **BDTSe-TTPD** was fully characterized by ^{1}H-NMR, ^{13}C-NMR and TOF-MS (Fig. S1-S6, ESI†).

BDTSe-TTPD with ethylhexyl selenophenes exhibits good solubility (> 15 mg/ mL) in tetrahydrofuran (THF), *o*-dichlorobenzene (*o*-DCB), chlorobenzene (CB) and chloroform (CF). The decomposion temperature (T_d) at 5% weight loss for **BDTSe-TTPD** was 419 ℃, as shown in Fig. S7, which provides sufficient thermal stablity for solar cell device fabrication.[15] Differential scanning calorimetry (DSC) was employed to study the thermal transitions of **BDTSe-TTPD**. As shown in Fig. S8, the melting temperature of the compound was observed to be 232 ℃ and an exothermic peaks at 203 ℃ was shown during cooling, which may be attributed to crystalline behavior.[16]

Optical properties

Fig. 1a shows the absorption spectra of pure **BDTSe-TTPD** in CF and in a thin film. The corresponding absorption data is summarized in Table 1. The solution absorption maximum (λ_{max}) located at 489 nm with a molar absorptivity of 34,520 L M^{-1} cm^{-1}. The film absorption was broadened and the λ_{max} was red-shifted to 528 nm with a shoulder increasing at a quite bathochromic-shifted wavelength of 573 nm, indicating strong π-π molecule stacking in the film state.[17] The optical bandgap (E_g^{opt}) calculated from the film absorption edge was 1.86 eV.

PL spectra of spin-cast films of pure **BDTSe-TTPD,** and of 1:2 (w/w) blends of the small molecules and $PC_{71}BM$, were examined to determine their charge transfer properties (Fig. 1b). **BDTSe-TTPD** showed a strong PL emission band with a maximum at 632 nm. Upon addition of $PC_{71}BM$, the emission band was almost completely quenched, suggesting ultrafast photoinduced charge transfer from the small molecule to PCBM.[18]

Fig. 1c shows the absorption of **BDTSe-TTPD**:$PC_{71}BM$ blended films mixed in a 1:1 weight ratio and spin-coated with *o*-DCB, CB or CF as the solvent, which were used in

implement in the device preparations. The blended films exhibited a full coverage from 300 to 700 nm, indicating the high light-harvesting ability of the active layer. Compared to the absorption of pure **BDTSe-TTPD**, the absorption band from 300 to 450 nm resulted mainly from the $PC_{71}BM$.[19] The overall relative absorbance strength in overall UV-visible range is increased based on the solvent in the following sequence: *o*-DCB < CB < CF. This result can be ascribed to the strong intermolecular interaction between small molecule and PCBM, [20] which provides higher order in the **BDTSe-TTPD** and $PC_{71}BM$ domains.

Electrochemical properties

Electrochemical cyclic voltammetry (CV) with a scan rate of 50 mV/s was employed to investigate the oxidation behavior of **BDTSe-TTPD** using a platinum counter electrode in an acetonitrile solution containing 0.1 mol L^{-1} Bu_4NPF_6 (Fig. 2a). The onset oxidation potential was 0.94 V vs. Ag/Ag^+. The corresponding highest occupied molecular orbital (HOMO) energy level of **BDTSe-TTPD** was estimated to be -5.34 eV, using the ferrocene reference value of -4.4 eV below the vacuum level.[21] The lowest unoccupied molecular orbital (LUMO) level was determined to be -3.48 eV, using the calculated HOMO value and the optical band gap. These energy levels match well with the acceptor material of $PC_{71}BM$, as shown in Fig. 2b.

To better understand the oxidative and reductive properties of **BDTSe-TTPD**, the geometry and electronic structure of **BDTSe-TTPD** were examined using Density Functional Theory. Becke's three parameter gradient corrected functional (B3LYP) with a polarized 6-31 G** basis was used for full geometry optimization. Methyl alkyl groups were used in place of the long alkyl substituents to limit computation time. The geometry and the HOMO and LUMO surface plots of the ground-state optimized structures are illustrated in Fig. 3. The HOMO is located predominantly on the BDT core, whereas the LUMO has both thiophene and TPD

character. The calculated HOMO and LUMO energies of the ground-state optimized geometry of **BDTSe-TTPD** were -5.03 eV and -2.58 eV, respectively, and the band gap was determined to be 2.45 eV.

Photovoltaic properties

To evaluate the photovoltaic performances of **BDTSe-TTPD**, we fabricated bulk heterojunction solar cells using **BDTSe-TTPD** as the donor material and $PC_{71}BM$ as the acceptor material with a traditional ITO/PEDOT:PSS/**BDTSe-TTPD**:$PC_{71}BM$/LiF/Al architecture (Fig. 4a). During the preliminary device optimization process, the effect of different **BDTSe-TTPD**:$PC_{71}BM$ active-layer compositions (from 1:0.5 to 1:4 weight ratio) cast from *o*-DCB was investigated. Current density voltage (*J-V*) characteristics under one sun (simulated AM1.5G irradiation at 100 mW cm^{-2}) are shown in Fig 4b and the photovoltaic parameters are summarized in Table 2. Optimal fabrication conditions were achieved using a **BDTSe-TTPD**-to-$PC_{71}BM$ ratio of 1:2 (w/w) which gave an open-circuit voltage (V_{oc}) of 0.92 V, a short-circuit current (J_{sc}) of 5.0 mA cm^{-2}, and a fill factor (FF) of 38.5 %, and a PCE of 1.86 % (Fig. 4b). Because **BDTSe-TTPD** has a low-lying HOMO energy level, it produced a high V_{OC} values in the solar cell devices.[22]

In order to study the effect of the solvents on the solar cell performance, thin films of **BDTSe-TTPD**:$PC_{71}BM$ (1:2) were prepared using *o*-DCB, CB, or CF. Fig. 4c shows the photocurrent densities of the solar cells in which the active layers were prepared with the different solvents. The corresponding performance parameters are summarized in Table 3.

The devices prepared using *o*-DCB and CB as solvents had a PCE = 1.86 % (V_{oc} = 0.92 V, J_{sc} = 5.30 mA cm^{-2}, and FF = 38.5%) and PCE = 2.98% (V_{oc} = 0.92 V, J_{sc} = 8.00 mA cm^{-2}, and FF = 40.5%), respectively, whereas the device spin-coated from CF demonstrated the best performance with PCE = 3.70% (V_{oc} = 0.92 V, J_{sc} = 10.00 mA cm^{-2}, and FF = 40.0%). The

best performance in the devices prepared by CF was mainly due to dramatically increased J_{SC}, which was attributed to strong light absorption and photo-response (conversion of input photons to photocurrent) as well as film morphology and nanostrucural order (film morphology and nanostructural order will be discussed below). **BDTSe-TTPD**:$PC_{71}BM$ films spin-coated from CF had higher light absorption than the films prepared from *o*-DCB and CB, which likely contributed to greater exciton and charge generation in the **BDTSe-TTPD**:$PC_{71}BM$ devices prepared using CF.[23] Moreover, the photo-response of the **BDTSe-TTPD**:$PC_{71}BM$ solar cells prepared using CF was over 58% at 540 nm, whereas that of the devices prepared from *o*-DCB and CB were over 36% at 530 nm and about 49% at 532 nm, respectively (Fig. 4d). The best EQE performance of the device spin-coated from CF can be attributed to greater conversion of input photons to photocurrent at all absorption wavelengths, which is consistent with the short circuit current observed.[24]

Fig. 5a shows the PCE thickness dependence of the active layer. To optimize the PCE of **BDTSe-TTPD**:$PC_{71}BM$ solar cells, the thicknesses of 75 nm, 95 nm, 130 nm, and 160 nm were prepared using different spin-coating conditions. The photovoltaic cell with the 95 nm thickness (1500 rpm for 40 s) exhibited an optimized PCE of 4.37% (V_{oc} = 0.90 V, J_{sc} = 10.5 mA cm^{-2} , and *FF* = 46.3 %). At a thickness of 160 nm, the PCE decreased to 2.61% (V_{oc} = 0.90 V, J_{sc} = 7.6 mA cm^{-2}, and *FF* = 38.2%). The **BDTSe-TTPD**:$PC_{71}BM$ solar cells have the tendency of having a reduced V_{oc}, J_{sc} and FF when the active-layer thickness is larger than 130 nm, as shown in Fig. 5b–d and Table 4.

Hole Mobility

Hole mobilities of the **BDTSe-TTPD**:$PC_{71}BM$ films, which were prepared from using *o*-DCB, CB, or CF were evaluated using the space charge limited current (SCLC) model. The experimental details are described in the Experimental section. As shown in Fig. 6, the

average hole mobilities for films casting from *o*-DCB, CB, and CF were found to be 2.22 × 10^{-7} cm^2/V s, 7.23 × 10^{-7} cm^2/V s, and 3.04 × 10^{-6} cm^2/V s, respectively, which is consistent with the trends in J_{SC} values. Compared to the *o*-DCB spin-coated device, the hole mobility of the CB spin-coated device improved, which is related to favorable nano-scale morphology with a distinct pathway. Devices prepared from CF showed a further improvement in hole mobility by an order of 3.04 × 10^{-6} cm^2/Vs, which is closely related to the intermolecular packing interaction as well as the charge stability when the exciton is separated, leading to an increase in the transporting property of hole carrier.[25]

Thin-film morphology

The surface morphology of the **BDTSe-TTPD**:$PC_{71}BM$ blended films, spin-coated from *o*-DCB, CB or CF were studied by atomic force microscopy (AFM). Fig. 7 shows the topographic images collected from the device films prepared with the three solvents. The *o*-DCB spin-coated films (a) exhibited a relatively formless and flat surface with a root-mean-squared (RMS) roughness of 0.75 nm. On the other hands, blended films spin-coated from CB showed weakly aggregated domains and shortly connected pathway.

When CF was used as the solvent (c), clear phase-separated, highly long path, and ordered networks with longer connected pathways and a large RMS roughness of 1.60 nm were observed. This most likely originated from the enhanced intermolecular interaction between the **BDTSe-TTPD** molecules[26] as was also evidenced by the optical properties and hole-mobilities. The improved short circuit current can clearly be examined through this better organized bulk heterojunction network structure, which is the key requirement of efficient charge separation and transport,[27] highly improved short circuit current can clearly be explained.

Molecule Stacking

In order to obtain insightful information concerning the molecular packing in the blended films with $PC_{71}BM$, X-ray diffraction (XRD) patterns (out-of-plane and in-plane) of the **BDTSe-TTPD**:$PC_{71}BM$ films, prepared using *o*-DCB, CB, or CF were compared (see Fig. 8). As shown in Fig. 8a, compared to the *o*-DCB spin-coated blend film, the CB spin-coated film shows longer-range crystalline structure, and contains a weak second order lamellar reflection (2θ = 3.41°) with a corresponding interlayer *d*-spacing distance of 18.02 Å. For the **BDTSe-TTPD**:$PC_{71}BM$ films prepared from CF, stronger crystalline diffraction peaks with second order diffraction of high intensity were observed, suggesting that the CF spin-coated film has much more crystalline order.[28] This findings, indicates the blended film prepared using CF were comprised of high-order **BDTSe-TTPD** crystallites and agrees well with the film morphology findings regarding crystallinity. Also, the presence of $PC_{71}BM$ can be clearly seen by the peak at 12.9° in the CF spin-coated film, which indicates that PCBM domains were more ordered.

For the in-plane XRD patterns (Fig. 8b), the trends in the diffraction patterns were similar to the out-of-plane and in-plane directions. It should be noted that the CF spin-coated film showed high-order crystalline planes and distinct π-π stacking diffraction (2θ = 17.12°, π-π stacking distance = 3.59 Å). However, the blended films prepared using *o*-DCB or CB exhibited diffractions without clear peaks or with very weak crystalline peaks, respectively, indicating that the **BDTSe-TTPD** crystallites were absent or had significantly weak intermolecular staking in the in-plain direction.[29] The dominant long-range ordering and strong π-π stacking of **BDTSe-TTPD** in the blended film prepared using CF enables efficient charge transport, which would explain; why devices spin-coated from CF showed an almost two-fold increase in PCE and had superior performance compared to those spin coated from the *o*-DCB and CB.[30]

Conclusions

A solution-processed small molecule solar cell based on alkylselenophene-substituted benzodithiophene, namely, **BDTSe-TTPD** was designed and synthesized. The A-D-A type molecule has broad absorption and has the HOMO level of -5.34 eV and the LUMO level of -3.48 eV, which both allign well with that of $PC_{71}BM$. Solvents including *o*-dichlorobenzene (*o*-DCB), chlorobenzene (CB) and chloroform (CF) were used for the spin-coating, to fabricate photovoltaic devices with **BDTSe-TTPD** as the donor material and $PC_{71}BM$ as the acceptor material. Finally, by using CF as the solvent, an optimized device with 95 nm active layer thickness was obtained, enabling a V_{OC} of 0.90 V, a J_{SC} of 10.5 mA/cm^2, a FF of 46.3%, and a PCE of 4.37%. Our results reveal that suitable molecular design (i.e., incorporation of the 2D conjugated selenophene unit in between two TPD moieties) and careful optimizations of the film morphologies by changing the spin-coating solvents will be one way toward highly efficient selenophene-based small molecule solar cells.

Experimental

Measurements and Characterizations

^{1}H-NMR spectra were recorded using a Bruker AM-200 spectrometer. ^{13}C-NMR spectra were measured on a Bruker Advance-300 spectrometer. HRMS (EI) spectra were performed on a high resolution GC mass spectrometer with LabRAM HR800 UV. Mass (MALDI-TOF/TOF) spectra were determined on a High resolution 4800 Tof/Tof mass spectrometer with Voyager DE-STR. The thermal analysis (TGA) were performed on a TA TGA 2100 thermogravimetric analyzer under a purified nitrogen with a heating rate of 10 °C/min. Differential scanning calorimetry (DSC) was conducted under nitrogen on a TA Instruments 2100 DSC. The sample was heated with 10 °C/min from 50 to 300 °C. UV-Vis absorption spectra were determined using a Carry 5000 UV-vis-near-IR double beam spectrophotometer.

Photoluminescence (PL) spectra were obtained using a FP-6500 (JASCO). Cyclic voltammetry (CV) was performed using a PowerLab/AD instrument model system in 0.1 M solution of tetrabutylammonium hexafluorophospate (Bu_4NPF_6) in anhydrous acetonitrile as supporting electrolyte at a scan rate of 50 mV/s. A glassy carbon disk (~0.05 cm^2) coated with a thin small molecule film, an Ag/AgCl electrode, and a platinum wire were used as working electrode, reference electrode, and counter electrode, respectively. Density functional theory (DFT) calculations were carried out at the B3LYP/6-31G* level of theory using the Spartan 08 computational programs. The atomic force microscope (AFM) (Multimode Ⅲa, Digital Instruments) was operated in tapping mode to obtain surface images (surface area: 5 × 5 μm^2) of the small molecule:PCBM blend films under ambient conditions. The X-ray diffraction (XRD) was performed at the 5A beamline (wavelength = 1.071 Å) at the Pohang Accelerator Laboratory (PAL) in Korea. The small molecule:PCBM blended films were prepared on a Si/PEDOT:PSS substrate by spin-coating method.

Fabrications and Characterizations of Organic Solar Cells

The devices were fabricated with a conventional structure of glass/ITO/PEDOT:PSS/active layer(**BDTSe-TTPD**:PCBM)/LiF/Al using a solution process. The ITO-coated glass substrates were cleaned by ultrasonic treatment in detergent, deionized water, acetone, and isopropyl alcohol under ultrasonication for 20 min each and subsequently dried by a nitrogen blow. A thin layer (~40 nm) of PEDOT:PSS (Clevios P VP AI 4083, filtered at 0.45μm PVDF) was spin-coated at 4000rpm onto the ITO surface. After being baked at 120 °C for 20min, the substrates were transferred into a nitrogen-filled glovebox. Subsequently, the active layer (~100 nm) was spin-coated from donor-acceptor blend solutions (40 mg/ml) with different ratios and solvents at 1000 rpm. Finally, a 0.8 nm LiF and 80 nm Al layer were deposited on the active layer under high vacuum (2 × 10^{-6} torr). The effective area of each cell was ~9 mm^2

defined by the mask. The current density-voltage (*J-V*) characteristics of photovoltaic devices were measured under ambient conditions, using a Keithley Model 2400 source-measurement unit. An Oriel xenon lamp (450 W) with an AM 1.5 G filter was used as the solar simulator. The light intensity was calibrated to 100 mW/cm^2, using a calibrated silicon cell with a KG5 filter, which is traced to the National Renewable Energy Laboratory (LREL). The external quantum efficiency (EQE) spectra were obtained by using a photomodulation spectroscopic set-up (model Merlin, Oriel), a calibrated Si UV detector, and a SR570 low noise current amplifier.

Hole mobility measurement

The hole only devices were fabricated with configuration of ITO/PEDOT:PSS/**BDTSe-TTPD**:$PC_{71}BM$/Au. The Au layer was deposited under a low speed (1 /s) to avoid the penetration of Au atoms into the active layer. The active layers were spin-coated with *o*-DCB, CB, and CF, respectively. Mobilities were extracted by fitting the current-voltage curves using the Mott-Curney relationship (space charge limited current).

$$J = \frac{9}{8}\varepsilon_0\varepsilon_r\mu_h\frac{V^2}{L^3}$$

Where J is the current density, L is the film thickness of active layer, μ_h is the hole mobility, ε_r is the relative dielectric constant of the transport medium, ε_0 is the permittivity of free space, V is the internal voltage in the device and $V = V_{appl} - V_r - V_{bi}$, where V_{appl} is the applied voltage to the device, V_r is the voltage drop due to contact resistance and series resistance across the electrodes, and V_{bi} is the built-in voltage due to the relative work function difference of the two electrodes. The V_{bi} can be determined from the transition between the ohmic region and the SCLC region.

Materials

N,N-Dimethylformamide (DMF), Tetrahydrofuran (THF), N-Bromosuccinimide (NBS), n-BuLi, toluene, chloroform, $Pd(PPh_3)_2Cl_2$, zinc powder and trimethyltin chloride were purchased from Aldrich, Alpha, and Langchem Inc. All these chemicals were used without further purification.

Synthesis of small molecule

2.5.1. 2-(2-ethylhexyl)selenophene (1)

To a solution of selenophene (30.00 g, 0.228 mol) in THF 400 mL was added a n-BuLi (109.20 mL, 2.5M in hexanes, 0.273 mol) at 0 °C. After 30 min, the mixture was cooled down −15 °C and 3-(bromomethyl)heptane (52.72 g, 0.273 mol) was added. The mixture was heated at 50 °C and stirred for 12 h. Then it was hydrolyzed with a saturated solution of NH_4Cl and extracted with diethyl ether. The organic layer was dried and evaporated, the residue was chromatography using silica gel column with Hexane/CH_2Cl_2 (20:1) as eluent to gave compound 1 (31.00 g, 56%). ^{1}H NMR (300 MHz, CD_2Cl_2) : δ = 7.85 (d, 1H), 7.16 (d, 1H), 6.96 (d, 1H), 2.88 (d, 2H), 1.42 (m, 1H), 1.39-1.30 (br, 8H), 0.93 (t, 6H).

2.5.2. 4,8-Bis(5-(2-ethylhexyl)selenophene-2-yl)benzo[1,2-b:4,5-b']dithiophene (2)

In a dried three-neck 250 mL nitrogen purged flask, n-BuLi (19.00 mL, 2.5 M in hexane, 0.047 mol) was added dropwise for 30 min to a mixture of compound 1 (12.00 g, 0.047 mol) in 100 mL THF at 0 °C. The mixture was then warmed to 50 °C and stirred for 2 h, after that 4,8-dehydrobenzo[l, 2-b:4, 5-b']dithiophene-4,8-dione (5.00 g, 0.022 mol) was subsequently added to the reaction mixture, which was then stirred for 1.5 h at 50 °C. After cooling the reaction mixture to ambient temperature, $SnCl_2{\cdot}2H_2O$ (6.00 g, 0.034 mmol) in 10 mL HCl (10%) was added and the mixture was stirred for additional 2 h, after which it was

subsequently poured into ice water and extracted with diethyl ether. The combined extracts were dried with anhydrous $MgSO_4/CH_2Cl_2$ (4:1) and then evaporated. The crude product was purified by column chromatography on silica gel eluting with Hexane to give pure compound 2 (8.00 g, 61%). ^{1}H NMR (300 MHz, $CDCl_3$), δ = 7.68 (d, 2H), 7.47 (d, 2H), 7.43 (d, 2H), 7.05 (d, 2H), 2.95 (d, 4H), 1.80 (m, 2H), 1.57–1.34 (br, 16H), 0.99–0.92 (m, 12H). ^{13}C NMR (500 MHz, $CDCl_3$): δ = δ = 145.73, 139.02, 137.24, 136.53, 127.70, 127.43, 125.35, 124.10, 123.41, 41.50, 34.29, 32.52, 28.94, 25.77, 23.01, 14.13, 10.91.

2.5.3. 2,6-Bis(trimethyltin)-4,8-bis(5-(2-ethylhexyl)selenophen-2-yl)benzo[1,2-b:4,5-b']dithiophene (3)

In a dry two-neck 100 mL nitrogen purged flask, compound 2 (1.50 g, 0.002 mol) was dissolved in 25 mL anhydrous THF. The solution was cooled to 0 °C, and a solution of n-BuLi (2.00 mL, 2.5 M in hexane, 0.004 mol) was added dropwise with stirring. The reaction mixture was then stirred for 2 h at room temperature. Next, the reaction mixture was cooled to 0 °C and a chlorotrimethylstannane (1.00 g, 0.004 mol) was added in one portion. The reaction mixture was stirred at 0 °C for 30 min and then warmed to room temperature for 2 h. Subsequently, the reaction mixture was quenched by the addition of 10 mL distilled water, and then the mixture was extracted by diethyl ether. Finally, the combined organic phase was dried with anhydrous $MgSO_4$ and concentrated to obtain yellow viscous crude product. Further purification was carried out by recrystallization with ethanol and ether to obtain the pure compound 3 (1.23 g, 87%). ^{1}H NMR (300 MHz, $CDCl_3$), δ = 7.72 (d, 2H), 7.44 (d, 2H), 7.06 (d, 2H), 2.95 (d, 4H), 1.68 (m, 2H), 1.57–1.35 (br, 16H), 1.00–0.91(m, 12H), 0.41-0.31 ppm (t, 18H).

2.5.4. 5-octyl-1, 3-di(thiophen-2-yl)-4H-thieno[3,4-c]pyrrole-4,6(5H)-dione (4)

The compound was synthesized by literature method.[31] Recrystallization from hexanes afforded compound 4 (4.88 g, 11.34 mmol, 64%). ^{1}H NMR (300 MHz, $CDCl_3$): δ = 8.00 (s, 2H), 7.45 (s, 2H), 7.15 (t, 2H), 3.68(t, 2H), 1.72 (m, 2H), 1.32 (m, 10H), 0.88 (t, 3H).

2.5.5. 1-(5-bromothiophen-2-yl)-5-octyl-3-(thiophen-2-yl)-4H-thieno[3,4-c]pyrrole-4,6(5H)-dione (5)

The compound was synthesized by literature method.[31] Recrystallization from hexanes afforded compound 10 (3.44 g, 6.78 mmol, 53%) as yellow solid. ^{1}H NMR (300 MHz, DMSO): δ = 7.99 (s, 1H), 7.83 (s, 1H), 7.70 (t, 1H), 7.35 (d, 1H), 7.24(d, 1H), 3.51(t, 2H), 1.50 (s, 2H), 1.27 (m, 10H), 0.84 (m, 3H).

*2.5.6. 3,3'-((4,8-bis(5-(2-ethylhexyl)selenophen-2-yl)benzo[1,2-b:4,5-b']dithiophene-2,6-diyl)bis(thiophene-5,2-diyl))bis(5-octyl-1-(thiophen-2-yl)-4H-thieno[3,4-c]pyrrole-4,6(5H)-dione) (**BDTSe-TTPD**)*

Compound 3 (0.98 g, 0.98 mmol) and compound 6 (1.10 g, 2.15 mmol) were dissolved in dry toluene 30 mL and degassed with nitrogen for 10 min. Then, $Pd(PPh_3)_2Cl_2$ (0.02 g, 0.03 mmol) was added. The mixture was stirred at 100 °C overnight under the nitrogen atmosphere. The reaction mixture was poured into water and extracted three times with chloroform. The organic phase was combined and dried over anhydrous magnesium sulfate. The residue was purified by column chromatography on silica gel (hexane/dichloromethane=1:1) to give **BDTSe-TTPD** (0.46 g, 31%). ^{1}H NMR (300 MHz, CD_2Cl_2), δ = 7.99 (d, 2H), 7.91 (d, 2H), 7.66 (s, 2H), 7.44 (t, 2H), 7.32(d, 2H), 7.24 (d, 2H), 7.13 (d, 2H), 6.97 (d, 2H), 3.68 (t, 4H), 2.95 (t, 4H), 1.70 (br, 8H), 1.57–1.29 (br, 34H), 1.07–0.97 (m, 18H). ^{13}C NMR (500 MHz, $CDCl_3$): δ 162.7, 162.6, 146.2, 140.6, 139.6, 137.4, 136.9, 135.9, 135.6, 132.9, 132.7, 132.2, 130.9, 130.2, 128.8, 128.7, 128.6, 128.4, 126.1,

125.9, 125.6, 123.6, 120.3, 41.8, 38.9, 34.8, 33.0, 32.2, 29.6, 29.4, 28.8, 27.5, 27.4, 26.2, 23.5, 23.0, 14.7, 14.4, 11.4. MS (MALDI-TOF/TOF): calculated for $C_{78}H_{84}N_2O_4S_8Se_2$, 1528.38;

Acknowledgements

This work was supported by the New & Renewable Energy of the Korea Institute of Energy Technology Evaluation and Planning (KETEP) grant funded by the Korea government Ministry of Knowledge Economy (No. 20123010010140)

† **Electronic supplementary information (ESI) available.** See DOI:~

Notes and references

1 (a) A. J. Heeger, *Chem. Soc. Rev*., 2010, **39**, 2354; (b) H. Zhou, L. Yang and W. You, *Macromolecules.*, 2012, **45**, 607; (c) P. M. Beaujuge and J. M. J. Fréchet, *J. Am. Chem. Soc*., 2011, **133**, 20009.

2 R. Lecover, N. Williams, N. Markovic, D. H. Reich, D. Q. Naiman, and H. E. Katz, *ACS Nano*., 2012, **6**, 2865.

3 J. You, L. Dou, K. Yoshimura, T. Kato, K. Ohya, T. Moriarty, K. Emery, C. –C. Chen, J. Gao, G. Li and Y. Yang, Nat. Comm., 2013, 1.

4 (a) Y. Sun, G. C. Welch, W. L. Leong, C. J. Takacs, G. C. Bazan and A. J. Heeger, *Nat. Mater*., 2012, **11**, 44; (b) A. K. K Kyaw, D. H. Wang, V. Gupta, J. Zhang, S. Chand, G. C. Bazan and A. J. Heeger, *Adv. Mater*., 2013, **25**, 2397.

5 (a) D. Ye, X. Li, L. Yan, W. Zhang, X. Hu, Y. Liang, J. Fang, W. –Y. Wong, and X. Wang, *J. Mater. Chem. A.,* 2013, **1**, 7622; (b) B. Walker, A. B. Tamayo, X. –D. Dang, P. Zalar, J. H. Seo, A. Garcia, M. Tantiwiwat and T. –Q. Nguyen, *Adv. Funct. Mater*., 2009, **19**, 3063; (c) Y. Liu, X. Wan, F. Wang, J. Zhou, G. Long, J. Tian, J. You, Y. Yang and Y. Chen, *Adv. Energy.*

Mater., 2011, **1**, 771.

6 J. Zhou, Y. Zuo, X. Wan, G. Long, Q. Zhang, W. Ni, Y. Liu, Z. Li, G. He, C. Li, B. Kan, M. Li, Y. Chen, *J. Am. Chem. Soc*., 2013, **135**, 8484.

7 A. Mishra and P. Bäuerle, *Angew. Chem. Int. Ed*., 2012, **51**, 2020.

8 Online publish

9 (a) Y. Li, *Acc. Chem. Res*., 2012, **45**, 723; (b) J. Yuan, Z. Zhai, H. Dong, J. Li, Z. Jiang, Y. Li and W. Ma, *Adv. Funct. Mater*., 2013, **23**, 885; (c) C. Cui, J. Min, C.-L. Ho, T. Ameri, P. Yang, Z. Zhao, C. J. Brabec and W. –Y. Wong, *Chem. Comm.,* 2013, **49**, 4409.

10 (a) S. Shen, P. Jiang, C. He, J. Zhang, P. Shen, Y. Zhang, Y. Yi, Z. Zhang, Z. Li and Y. Li, *Chem. Mater*., 2013, **25**, 2274; (b) C. Cui, W. –Y. Wong and Y. Li, *Energy Environ. Sci.*, 2014, DOI: 10.1039/C4EE00446A.

11 (a) I. Kang, T. K. An, J. -a. Hong, H. –J. Yun, R. Kim, D. S. Chung, C. E. Park, Y. –H. Kim, and S. –K. Kwon, *Adv. Mater*., 2013, **25**, 524. (b) S. Haid, A. Mishra, M. Weil, C. Uhrich, M. Pfeiffer and P. Bäuerle, *Adv. Funct. Mater*., 2012, **22**, 4322; (c) M. Shahid, R. S. Ashraf, Z. Huang, A. J. Kronemeijer, T. M-Ward, I. McCulloch, J. R. Durrant, H. Sirringhaus and M. Heeney, *J. Mater. Chem*., 2012, **22**, 12817.

12 H. A. Saadeh, L. Lu, F. He, J. E. Bullock, W. Wang, B. Carsten and L. Yu, *ACS Macro Lett*., 2012, **1**, 361.

13 D. H. Wang, A. Pron, M. Leclerc and A. J. Heeger, *Adv. Funct. Mater*., 2013, **23**, 1297.

14 B. Kim, H. R. Yeom, M. H. Yun, J. Y. Kim and C. Yang, *Macromolecules.,* 2012, **45**, 8658.

15 H. Bai, P. Cheng, Y. Wang, L. Ma, Y. Li, D. Zhu and X. Zhan, *J. Mater. Chem. A*., 2014, **2**, 778.

16 X. Liu, Y. Sun, L. A. Perez, W. Wen, M. F. Toney, A. J. Heeger and G. C. Bazan, *J. Am. Chem. Soc*., 2012, **134**, 20609.

17 (a) W. Li, K. H. Hendriks, A. Furlan, W. S. C. Roelofs , S. C. J. Meskers, M. M. Wienk,

and R. A. J. Janssen, *Adv. Mater*., 2013; (b) G. W. P. v. Pruissen, E. A. Pidko, M. M. Wienk and R. A. J. Janssen, *J. Mater. Chem. C*., 2014, **2**, 731.

18 R. Shivanna, S. Shoaee, S. Dimitrov, S. K. Kandappa, S. Rajaram, J. R. Durrant and K. S. Narayan, *Energy Environ. Sci*., 2014, **7**, 435.

19 Y. Zou, A. Najari, P. Berrouard, S. Beaupre´, B. R. Aïch, Y. Tao and M. Leclerc, *J. Am. Chem. Soc*. 2010, **132**, 5330.

20 (a) J. Huang, C. Zhan, X. Zhang, Y. Zhao, Z. Lu, H. Jia, B. Jiang, J. Ye, S. Zhang, A. Tang, Y. Liu, Q. Pei and J. Yao, *ACS Appl. Mater. Interfaces*., 2013, **5**, 2033; (b) R. B. Aïch, Y. Zou, M. Leclerc and Y. Tao, Org. Elec., 2010, 11, 1053.

21 M. C. Hwang, J. -W. Jang, T. K. An, C. E. Park, Y. -H. Kim and S. -K. Kwon, *Macromolecules*, 2012, **45**, 4520.

22 L. Dou, J. You, J. Yang, C. –C. Chen, Y. He, S. Murase, T. Moriarty, K. Emery, G. Li and Y. Yang, *Nat. Photonics*., 2012, **6**, 180.

23 Z. He, C. Zhong, S. Su, M. Xu, H. Wu, Y. Cao, *Nat. Photonics*., 2012, **6**, 591.

24 T. –Y. Chu, J. Lu, S. Beaupré, Y. Zhang, J. –R. Pouliot, J. Zhou, A. Najari, M. Leclerc and Y. Tao, *Adv. Funct. Mater*., 2012, **22**, 2345.

25 (a) W. Wen, L. Ying, B. B. Y. Hsu, Y. Zhang, T. –Q. Nguyen and G. C. Bazan, *Chem. Commun*., 2013, **49**, 7192; (b) J. Min, Y. N. Luponosov, A. Gerl, M. S. Polinskaya, S. M. Peregudova, P. V. Dmitryakov, A. V. Bakirov, M. A. Shcherbina, S. N. Chvalun, S. Grigorian, N. Kaush-Busies, S. A. Ponomarenko, T. Ameri and C. J. Brabec, *Adv. Energy Mater*., 2013.

26 Q. Shi, P. Cheng, Y. Li, X. Zhan, *Adv. Ener. Mater*., 2012, **2**, 63.

27 J. D. Zimmerman, X. Xiao, C. K. Renshaw, S. Wang, V. V. Diev, M. E. Thompson and S. R. Forrest, *Nano. Lett*., 2012, **12**, 4366.

28 Y. –C. Huang, C. –S. Tsao, C. –M. Chuang, C. –H. Lee, F. –H. Hsu, H. –C. Cha, C. –Y. Chen, T. –H. Lin, C. –J. Su, U. –S. Jeng, W. –F. Su, *J. Phys. Chem. C*., 2012, **116**, 10238.

29 I. Osaka, M. Shimawaki, H. Mori, I. Doi, E. Miyazaki, T. Koganezawa, K. Takimiya, *J. Am. Chem. Soc*., 2012, **134**, 3498.

30 a) A. T. Yiu, P. M. Beaujuge, O. P. Lee, C. H. Woo, M. F. Toney and J. M. Frechet, *J. Am. Chem. Soc*. 2012, **134**, 2180; b) H. –Y. Chen, J. Hou, A. E. Hayden, H. Yang, K. N. Houk and Y. Yang, *Adv. Mater*., 2010, **22**, 371.

31 a) C. B. Nielsen and T. Bjornholm, *Org. Lett*., 2004, **19**, 3381; b) G. Sotgiu, M. Zambianchi, G. Barbarella and C. Botta, Tetrahedron., 2002, **58**, 2245; c) J. Yuan, X. Huang, H. Dong, J. Lu, T. Yang, Y. Li, A. Gallagher and W. Ma, Org. Elec., 2013, **14**, 635.

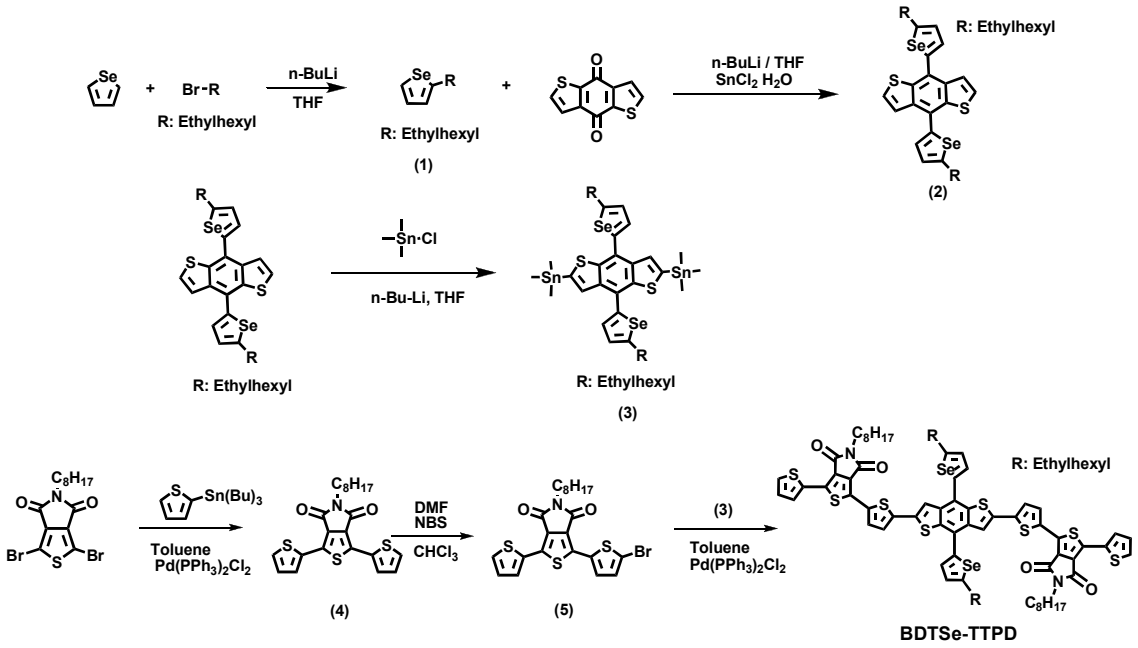

Scheme 1. Synthetic route to **BDTSe-TTPD**

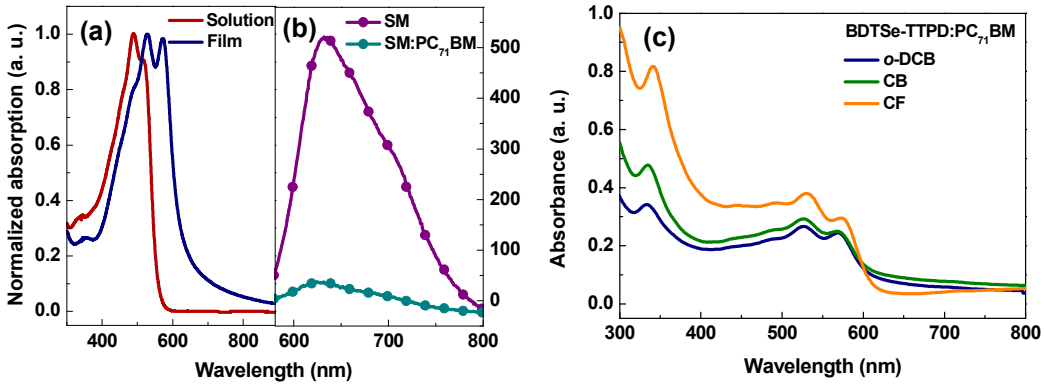

Fig 1. (a) UV-vis absorption spectra of pure **BDTSe-TTPD** in solution and film, (b) PL spectra of **BDTSe-TTPD** and **BDTSe-TTPD**:$PC_{71}BM$ (1:2) blend film, and (c) the blended film absorption of **BDTSe-TTPD** (1:1, weight ratio), prepared using different solvents.

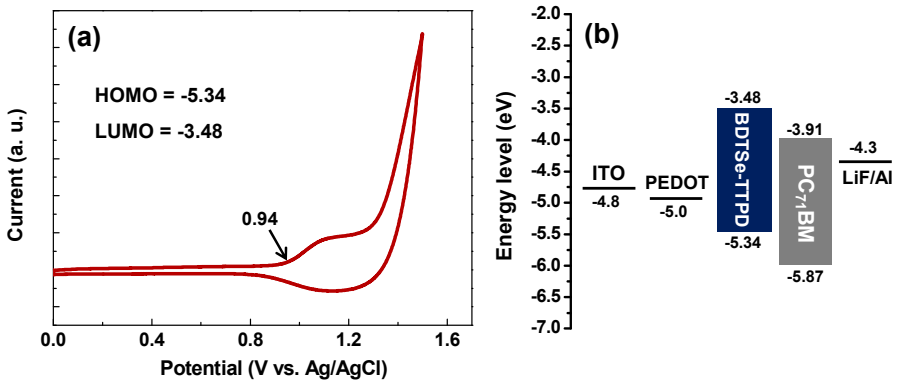

Fig. 2. (a) Cyclic voltammograms of **BDTSe-TTPD**, and (b) energy levels of different components in a photovoltaic device.

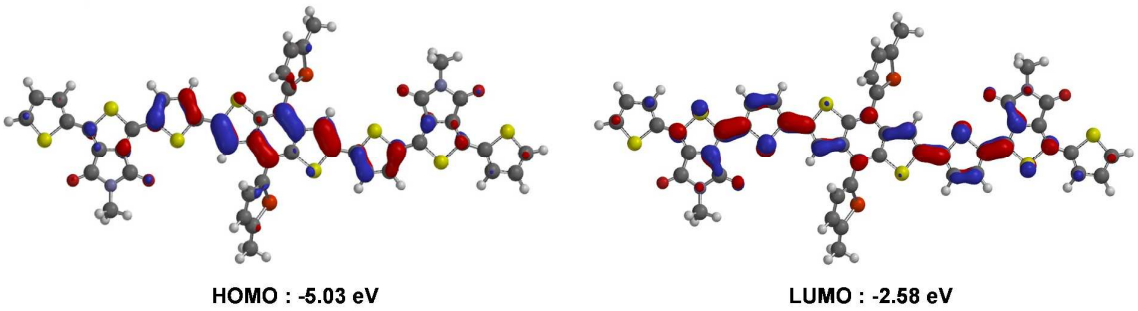

Fig. 3. HOMO and LUMO surface plots for **BDTSe-TTPD**

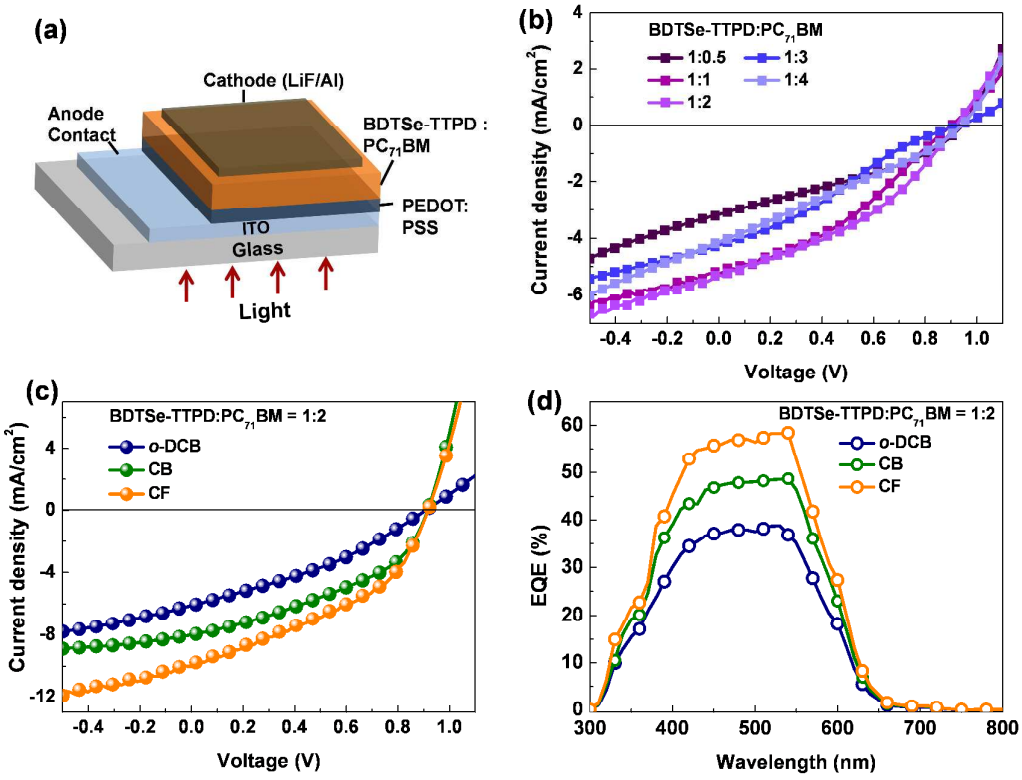

Fig. 4. (a) Schematic diagram of the photovoltaic cells. (b)-(c) *J*-*V* curves of different **BDTSe-TTPD**:$PC_{71}BM$ blend ratio and solvents, repectively. (d) External quantum efficiency (EQE) spectra of corresponding **BDTSe-TTPD**:$PC_{71}BM$ solar cells.

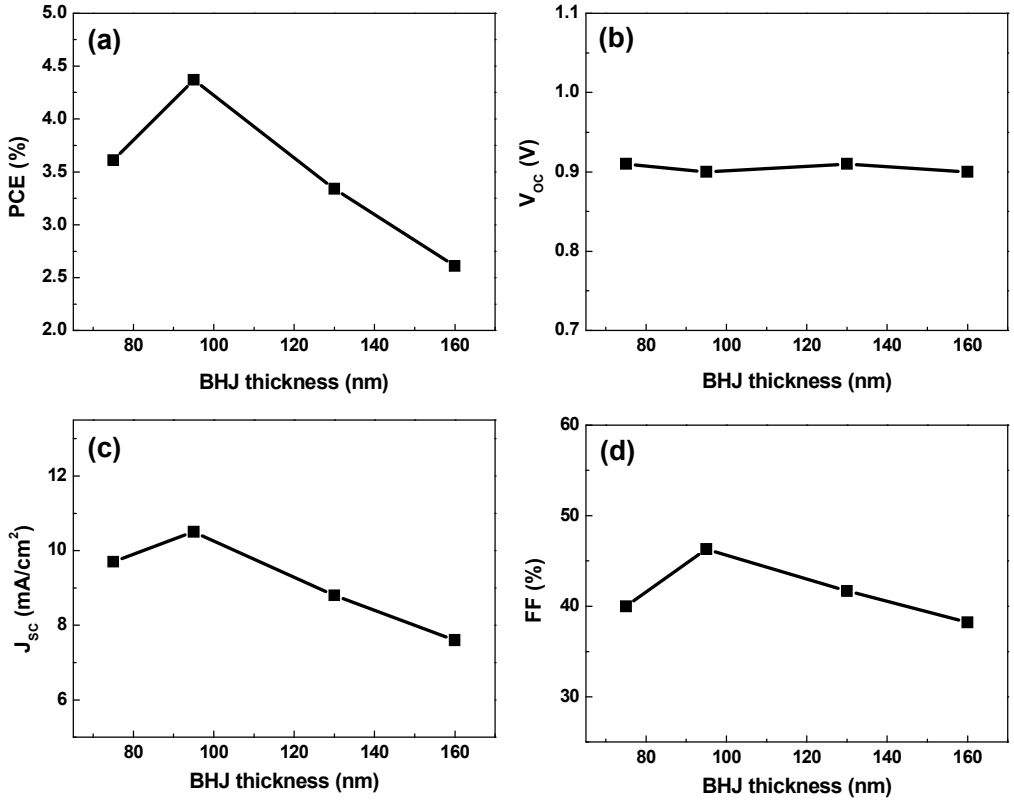

Fig. 5. (a) PCE as a function of the thickness of the active layer. (b) V_{OC}, (C) J_{SC}, and (d) FF of the **BDTSe-TTPD**:$PC_{71}BM$ BHJ solar cells depending on the various active-layer thickness.

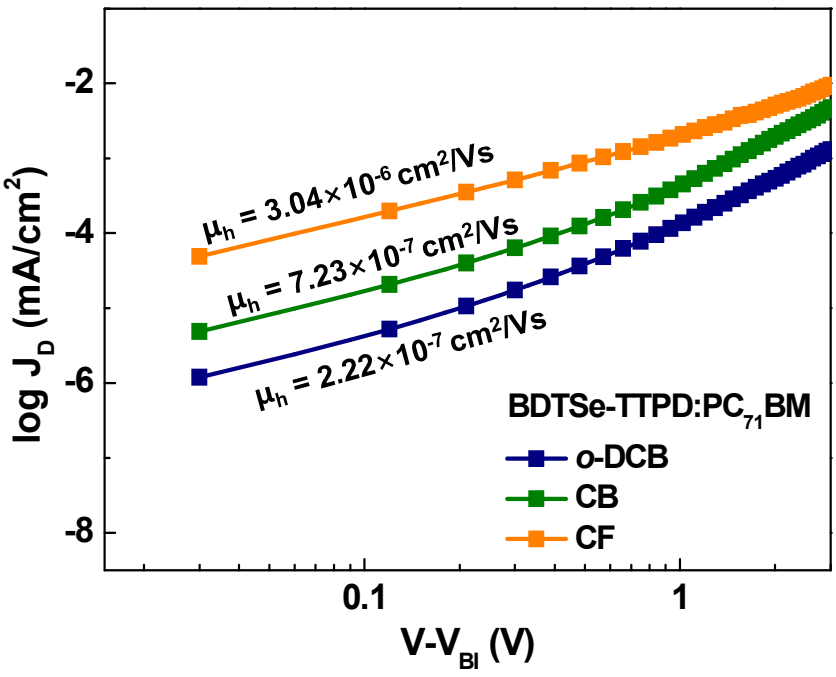

Fig. 6. Hole mobilities of the **BDTSe-TTPD**:$PC_{71}BM$ prepared from *o*-DCB, CB, CF, respectively.

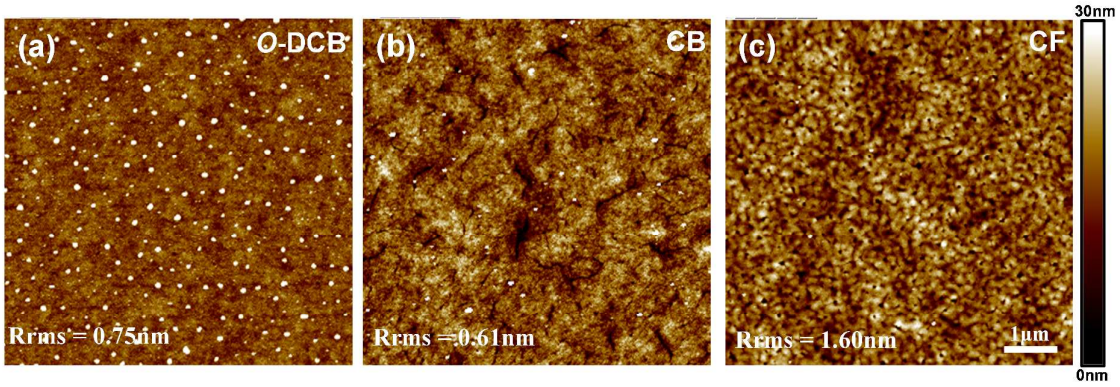

Fig. 7. AFM topographic images of the **BDTSe-TTPD**:$PC_{71}BM$ blended films prepared from (a) *o*-DCB, (b) CB, and (c) CF, respectively.

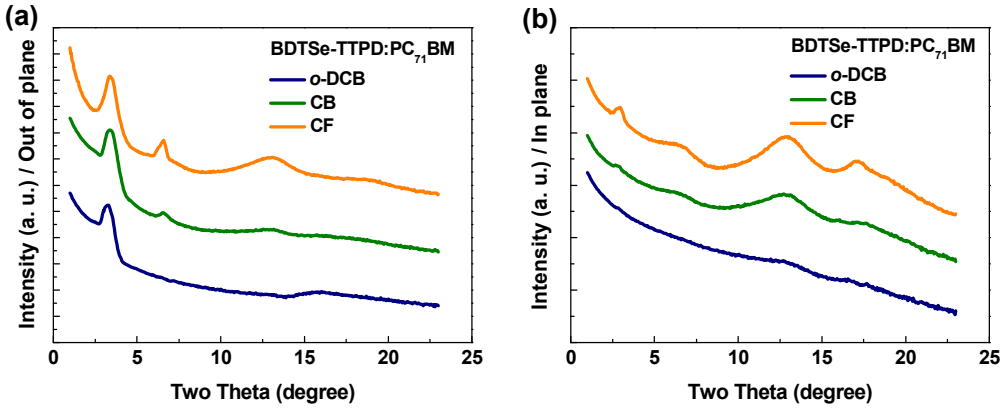

Fig. 8. Out-of-plane (a) and in-plane (b) XRD patterns of **BDTSe-TTPD**:$PC_{71}BM$ blend films prepared from different solvents.

Table 1. Optical, electrochemical and thermal properties of **BDTSe-TTPD**

Small Molecule	T_d (°C) [a]	T_m (°C) [b]	T_c (°C) [c]	ε_{max} / 10^3 solution	λ_{max} (nm) solution	λ_{max} (nm) film	λ_{onset} (nm) film	E_g^{opt} (eV) [d]
BDTSe-TTPD	419	232	203	34,520	489, 518	528, 573	665	1.86

[a] Decomposition temperature corresponding to 5% weight loss in N_2 determined by TGA.
[b] Melting temperature determined from DSC.
[c] Crystallization temperature determined from DSC.
[d] Estimated from the absorption edge in film ($E_g^{opt} = 1240/\lambda_{onset}$ eV).

Table 2. Device processing conditions and efficiency parameters of **BDTSe-TTPD**:$PC_{71}BM$ solar cells with various donor and acceptor blend ratios.

Small molecule : PCBM	Blend ratios	*V*oc (V)	*J*sc (mA / cm^2)	FF (%)	PCE (%)
BDTSe-TTPD : $PC_{71}BM$	1:0.5	0.92	3.2	34.3	1.01
	1:1	0.91	5.0	35.2	1.67
	1:2	0.92	5.3	38.5	1.86
	1:3	0.92	4.2	30.9	1.20
	1:4	0.93	4.1	27.8	1.15

Table 3. Performance parameters of **BDTSe-TTPD**:$PC_{71}BM$ solar cells of different solvents.

Small molecule : PCBM	Solvent	*V*oc (V)	*J*sc (mA / cm^2)	FF (%)	PCE (%)
BDTSe-TTPD : $PC_{71}BM$	*O*-DCB	0.92	5.3	38.5	1.86
	CB	0.92	8.0	40.5	2.98
	CF	0.92	10.0	40.0	3.70

Table 4. Device efficiency parameters of the **BDTSe-TTPD**:$PC_{71}BM$ solar cells, which depend on the active layer thicknesses, at a blend ratio of 1:2.

Small molecule : PCBM	Thickness (nm)	*V*oc (V)	*J*sc (mA / cm^2)	FF (%)	PCE (%)
BDTSe-TTPD : $PC_{71}BM$	75	0.91	9.7	40.8	3.61
	95	0.90	10.5	46.3	4.37
	130	0.91	8.8	41.7	3.34
	160	0.90	7.6	38.2	2.61